

V.F. LOS,¹ M.V. LOS²¹ Institute for Magnetism, Nat. Acad. Sci. of Ukraine
(36-b, Vernadsky Blvd., Kyiv 142, Ukraine)² Luxoft Eastern Europe
(14, Vasylkivs'ka Str., B, Business Center STEND, Kyiv 03040, Ukraine)AN EXACT SOLUTION OF THE TIME-DEPENDENT
SCHRÖDINGER EQUATION WITH A RECTANGULAR
POTENTIAL FOR REAL AND IMAGINARY TIMES

UDC 539

A propagator for the one-dimensional time-dependent Schrödinger equation with an asymmetric rectangular potential is obtained, by using the multiple-scattering theory. It allows the consideration of the reflection and transmission processes as the scattering of a particle at the potential jump (in contrast to the conventional wave-like picture) and the account for the non-classical counterintuitive contribution of the backward-moving component of the wave packet attributed to a particle. This propagator completely resolves the corresponding time-dependent Schrödinger equation (defines the wave function $\psi(x, t)$) and allows the consideration of the quantum mechanical effects of a particle reflection from the potential downward step/well and a particle tunneling through the potential barrier as a function of the time. These results are related to fundamental issues such as measuring the time in quantum mechanics (tunneling time, time of arrival, dwell time). For the imaginary time, which represents an inverse temperature ($t \rightarrow -i\hbar/k_B T$), the obtained propagator is equivalent to the density matrix for a particle that is in a heat bath and is subject to the action of a rectangular potential. This density matrix provides information about particles' density in the different spatial areas relative to the potential location and on the quantum coherence of different particle spatial states. If one passes to the imaginary time ($t \rightarrow -it$), the matrix element of the calculated propagator in the spatial basis provides a solution to the diffusion-like equation with a rectangular potential. The obtained exact results are presented as the integrals of elementary functions and thus allow a numerical visualization of the probability density $|\psi(x, t)|^2$, the density matrix, and the solution of the diffusion-like equation. The results obtained may also be applied to spintronics due to the fact that the asymmetric (spin-dependent) rectangular potential can model the potential profile in layered magnetic nanostructures.

Key words: Schrödinger equation, asymmetric rectangular potential, layered magnetic nanostructures.

1. Introduction

We start with the one-dimensional Schrödinger equation for a particle of mass m subject to a potential $V(x)$:

$$i\hbar \frac{\partial \psi(x; t)}{\partial t} = H\psi(x; t), \quad (1)$$

where H is a self-adjoint operator,

$$H = -\frac{\hbar^2}{2m} \frac{\partial^2}{\partial x^2} + V(x). \quad (2)$$

A solution to this equation can generally be presented as

$$\psi(x; t) = \int \langle x | K(t) | x' \rangle \psi(x'; 0) dx', \quad (3)$$

where $K(t) = \exp(-iHt/\hbar)$ is the propagator

(Green's function) for Eq. (1) in the operator form, and $\langle x|K(t)|x' \rangle$ is its matrix element in the x -representation. Thus, the knowledge of the propagator provides the complete solution to Eq. (1) at the given initial value of $\psi(x'; 0)$. If the initial value is of the form $\psi(x'; 0) = \delta(x' - x'')$, solution (3) reduces to the Green function matrix element

$$\psi(x, x''; t) = \langle x|K(t)|x'' \rangle. \quad (4)$$

Equation (1) with the imaginary time variable is also relevant to other physical situations. If we make the substitutions $t \rightarrow -i\hbar\beta$ ($\beta = 1/k_B T$) and $\psi(x, x'; -i\hbar\beta) \rightarrow \rho(x, x'; \beta)$, Eq. (4) represents the matrix element $\rho(x, x'; \beta) = \langle x|\exp(-\beta H)|x' \rangle$ of the density operator $\rho(\beta) = \exp(-\beta H)$, which satisfies the Bloch equation (in the x -representation)

$$\frac{\partial \rho(x, x'; \beta)}{\partial \beta} = -H\rho(x, x'; \beta), \quad (5)$$

with the initial condition $\rho(x, x'; \beta = 0) = \delta(x - x')$. In Eq. (5), the operator H (2) is applied only to the x variable of the density matrix.

If we make the substitutions $t \rightarrow -it$, $\hbar \rightarrow 2mD$, $V(x)/2mD \rightarrow \bar{V}(x)$, and $\psi(x; -it) \rightarrow Q(x; t)$, Eq. (1) represents the inhomogeneous diffusion-like equation (with the diffusion coefficient D)

$$\frac{\partial Q(x; t)}{\partial t} = D \frac{\partial^2 Q(x; t)}{\partial x^2} - \bar{V}(x)Q(x; t). \quad (6)$$

The solution to Eq. (6) at the initial condition $Q(x; 0) = \delta(x - x_0)$ is given by (4):

$$Q(x, x_0; t) = \langle x|\exp(-Ht/2mD)|x_0 \rangle, \quad (7)$$

where H is defined by (2) with $\hbar \rightarrow 2mD$.

We see that, in any case, the problem is to find a propagator of the type $\langle x|\exp(-\alpha H)|x' \rangle$ with different α for the considered parabolic differential equations.

A rectangular potential is the simplest one allowing the study of some striking quantum mechanical effects such as the particle reflection from a potential step/well and the transmission through a potential barrier. These phenomena are less surprising, when we think of a wave being, e.g., reflected from a downward potential step, though they are more surprising from the particle point of view. They easily follow from the standard textbook stationary analysis,

which reduces to substituting a plane wave with energy E for the wave packet and solving the stationary Schrödinger equation. However, in this case, there are no real transport phenomena, i.e. in the absence of the energy dispersion ($\Delta E = 0$), the transmission time through or the time of arrival (TOA) to the potential jumps is indefinite ($\Delta t \sim \hbar/\Delta E$). It is of interest to verify the mentioned non-classical phenomena by considering the time-dependent picture of these processes in a realistic situation, when a particle, originally localized outside the potential well/barrier, moves toward the potential and experiences the scattering at the potential jumps. In order to do this, the corresponding time-dependent Schrödinger equation needs to be solved. This problem is much more involved even in the one-dimensional case in comparison to the conventional stationary case.

In particular, there is one striking and classically forbidden counterintuitive (and often overlooked) effect even in the process of the simplest 1D time-dependent scattering by the mentioned potentials. A wave packet representing an ensemble of particles, confined initially (at $t = t_0$), say, somewhere to the region $x < 0$, consists of both positive and negative momentum components due to the fact that a particle cannot be completely localized at $x < 0$ if the wave packet contains only $p > 0$ components. One would then expect that only the particles with positive momenta p may arrive at positive positions $x > 0$ at $t > t_0$. However, wave packet's negative momentum components (restricted to a half-line in the momentum space) are necessarily different from zero in the whole x space ($-\infty \div \infty$), representing the presence of particles at $x > 0$ at the initial time moment t_0 and, therefore, may contribute, for example, to the distribution of the time of arrival (TOA) of particles to $x > 0$ [1, 2]. It is worth noting that the contribution of the backward-moving (negative momentum) components in the initial-value problem is, in some sense, equivalent to the contribution of the negative energy (evanescent) components in the source solution [1]. Thus, the proper treatment of some aspects of the kinetics of a wave packet (even in the 1D case and even for a "free" motion) becomes a nontrivial problem and is closely related to the fundamental problem of measuring the time in quantum mechanics, such as TOA, dwell time, and tunneling time.

In addition, the time-dependent aspects of the reflection from and transmission through the potential

step/barrier/well have recently acquired relevance not only in view of the renewed interest in the fundamental problems of measuring the time in quantum mechanics (see [3, 4]), but also due to important practical applications in the newly emerged fields of nanoscience and nanotechnology. Rectangular (asymmetric spin-dependent) potential barriers/wells may often satisfactorily approximate the one-dimensional potential profiles in layered magnetic nanostructures (with sharp interfaces). In such nanostructures, the giant magnetoresistance (GMR) [5] and tunneling magnetoresistance (TMR) [6] effects occur.

The calculation of the propagator $\langle x | \exp(-\alpha H) | x' \rangle$ is conveniently related to the path-integral method (see, e.g., [7] and [8]). The list of the exact solutions for this propagator is very short. For example, there is an exact solution for the space-time propagator $\langle x | \exp(-iHt/\hbar) | x' \rangle$ of the Schrödinger equation in the one-dimensional square barrier case obtained in [9], but this solution is very complicated, implicit, and not easy to analyze (see also [10–12]).

Recently, we have suggested a simple method for the calculation of the space-time propagator [13–15], which exactly resolves the time-dependent Schrödinger equation with a rectangular potential in terms of integrals of elementary functions. This method is an alternative to the commonly used path-integral approach to the mentioned problems and is based on the energy integration of the spectral density matrix (discontinuity of the energy-dependent Green function across the real energy axis). The energy-dependent Green function is then easily obtained for the step/barrier/well potentials within the multiple-scattering theory (MST), by using the effective energy-dependent potentials found in [13], which are responsible for the reflection from and the transmission through a potential step. These potentials, which are defined via the different particle velocities from both sides of the potential steps making up the step/barrier/well potentials, allow the consideration of the reflection and transmission processes as the particle scattering at the potential jumps in contrast to the conventional wave-like picture. An important advantage of our approach is that the negative energy (evanescent states) contribution to the propagator cancels out due to the natural decomposition of the propagator into forward- and backward-moving components. This is an essential result, because the accounting for both of these components (which should

generally be done) often leads to a rather complicated consideration of the evanescent states with $E < 0$ (see [16]).

In this paper, we provide an exact solution to Eq. (1) for real and imaginary times using our approach [13–15] to the calculation of the space-time propagator for a general asymmetric rectangular potential. In Section 2, we outline our MST approach to the calculation of the propagator for the time-dependent Schrödinger equation and present its explicit form. In Section 3, we consider a system in a heat bath, as is the case, e.g., for electrons in nanostructures. The equilibrium characteristics of the system can then be calculated knowing its density matrix $\rho(x, x'; \beta) = \langle x | \exp(-\beta H) | x' \rangle$. In that section, we present an exact solution for the density matrix of a particle in an asymmetric (spin-dependent) one-dimensional rectangular potential and discuss its properties with the help of a numerical evaluation of the corresponding integrals of elementary functions. In accordance with the above discussion of Eq. (1), the obtained solution for the space-time propagator may be also used for finding the solution to the diffusion-like equation (1) through the appropriate change of the parameters. This case is discussed in Section 4, and the summary of the results is given in Section 5.

2. Multiple Scattering Calculation of a Space-Time Propagator for the Schrödinger Equation

We start by considering a particle (electron) of mass m in the following general asymmetric one-dimensional rectangular potential of width d placed in the interval $0 < x < d$

$$V(x) = [\theta(x) - \theta(x - d)]U + \theta(x - d)\Delta, \quad (8)$$

where $\theta(x)$ is the Heaviside step function, and the potential parameters U and Δ can acquire positive, as well as negative, values (for $\Delta = U$, $V(x)$ reduces to the step potential). As an application, we can model a spin-dependent potential profile of the three-layer system made of a nonmagnetic spacer (metallic one or an insulator) sandwiched between two magnetic (infinite) layers by potential (8). The asymmetry (spin-dependence) of potential (8) is defined by the parameter Δ . The particle wave vectors in different spatial areas (layers) are defined as

$$k_{<}^0(E) = k(E), k(E) = \sqrt{\frac{2m}{\hbar^2}E}, x < 0,$$

$$\begin{aligned}
 k_{>}^0(E) &= k_{<}^d(E) = k_u(E), \\
 k_u(E) &= \sqrt{\frac{2m}{\hbar^2}(E - U)}, 0 < x < d, \\
 k_{>}^d(E) &= k_{\Delta}(E), k_{\Delta}(E) = \sqrt{\frac{2m}{\hbar^2}(E - \Delta)}, x > d. \quad (9)
 \end{aligned}$$

In the case of three-dimensional sandwiches, $k_{>}^0(E)$ and $k_{<}^d(E)$ are the perpendicular-to-interface components of the wave vector \mathbf{k} of a particle arriving at the interfaces (located at $x = 0$ and $x = d$) from the right ($>$) or from the left ($<$).

The wave function of a single particle moving in the perturbing potential $V(x)$ is given by Eq. (3) (see also [7]). The propagator $K(x, x'; t) = \langle x | \exp(-iHt/\hbar) | x' \rangle$ is the probability amplitude for the particle transition from the initial space-time point $(x', 0)$ to the final point (x, t) by means of all possible paths. It provides the full information about particle's dynamics and resolves the corresponding time-dependent Schrödinger equation (1). According to [13], the time-dependent retarded propagator $K(t) = \theta(t - t') \exp(-\frac{i}{\hbar}Ht)$ can be represented as

$$\begin{aligned}
 K(t) &= \theta(t) \frac{i}{2\pi} \int_{-\infty}^{\infty} dE e^{-\frac{i}{\hbar}Et} \times \\
 &\times \left(\frac{1}{E - H + i\varepsilon} - \frac{1}{E - H - i\varepsilon} \right), \quad \varepsilon \rightarrow +0, \quad (10)
 \end{aligned}$$

where H is the time-independent Hamiltonian of the system under consideration. Equation (10) follows either from the contour integration in the complex plane or from the identity

$$\frac{1}{E - H \pm i\varepsilon} = P \frac{1}{E - H} \mp i\pi\delta(E - H), \quad (11)$$

where P is the symbol of the integral principal value. In the space representation, (10) reads

$$K(x, x'; t) = \theta(t) \int_{-\infty}^{\infty} e^{-\frac{i}{\hbar}Et} A(x, x'; E) dE. \quad (12)$$

Here, $A(x, x'; E)$ is the spectral density matrix

$$\begin{aligned}
 A(x, x'; E) &= \frac{i}{2\pi} [G^+(x, x'; E) - G^-(x, x'; E)], \\
 G^+(x, x'; E) &= \langle x | \frac{1}{E - H + i\varepsilon} | x' \rangle, \\
 G^-(x, x'; E) &= [G^+(x', x; E)]^*, \varepsilon \rightarrow +0, \quad (13)
 \end{aligned}$$

determined by the matrix elements of the retarded $G^+(E)$ and advanced $G^-(E)$ energy-dependent operator Green functions $G^{\pm} = (E - H \pm i\varepsilon)^{-1}$, which

are analytic in the upper and lower half-planes of the complex energy E , respectively. The propagator in the form of (12) is a useful tool for calculations within the multiple-scattering theory (MST) perturbation expansion, if the Hamiltonian can be split as $H = H_0 + H_i$, where H_0 describes a free motion and H_i is the scattering potential. Note that, in this case, one would not need rely on the standard (often cumbersome) matching procedure characteristic of the picture, when a wave (representing a particle) is reflected from and transmitted through the potential (8). On the other hand, the introduction of the scattering potential H_i corresponds to the natural picture of the particle scattering at the potential jumps at $x = 0$ and $x = d$.

We showed in [13] that the Hamiltonian corresponding to the energy-conserving processes of scattering at potential steps can be presented as

$$\begin{aligned}
 H &= H_0 + H_i(x; E), \\
 H_i(x; E) &= \sum_s H_i^s(E) \delta(x - x_s). \quad (14)
 \end{aligned}$$

Here, $H_i(x; E)$ describes the perturbation of the "free" particle motion (defined by $H_0 = -\frac{\hbar^2}{2m} \frac{\partial^2}{\partial x^2}$) localized at the potential steps with coordinates x_s (in the case of potential (8), there are two potential steps at $x_s = 0$ and $x_s = d$)

$$\begin{aligned}
 H_{i>}^s(E) &= \frac{i\hbar}{2} [v_{>}^s(E) - v_{<}^s(E)], \\
 H_{i<}^s(E) &= \frac{i\hbar}{2} [v_{<}^s(E) - v_{>}^s(E)], \\
 H_{i><}^s(E) &= \frac{2i\hbar v_{>}^s(E) v_{<}^s(E)}{[\sqrt{v_{>}^s(E)} + \sqrt{v_{<}^s(E)}]^2}, \quad (15)
 \end{aligned}$$

where $H_{i><}^s(E)$ is the reflection (from the potential step at $x = x_s$) potential amplitude, the index $>$ ($<$) indicates the side, on which the particle approaches the interface at $x = x_s$: right ($>$) or left ($<$); $H_{i>}^s(E)$ is the transmission potential amplitude, and the velocities $v_{><}^s(E) = \hbar k_{><}^s(E)/m$, $s \in \{0, d\}$ ($k_{><}^s(E)$ are given by (9)).

The perturbation expansion for the retarded Green function $G^+(x, x'; E)$ in the case of the rectangular potential (8), which can be efficiently represented by the two-step effective scattering Hamiltonian (14), reads for different source (given by x') and destination (determined by x) areas of interest as follows:

$$G^+(x, x'; E) = G_0^+(x, d; E) T^+(E) G_0^+(0, x'; E),$$

$$\begin{aligned}
 & x' < 0, \quad x > d, \\
 & G^+(x, x'; E) = G_0^+(x, 0; E)T^+(E)G_0^+(d, x'; E), \\
 & x' > d, \quad x < 0, \\
 & G^+(x, x'; E) = G_0^+(x, 0; E)T'^+(E)G_0^+(0, x'; E) + \\
 & + G_0^+(x, d; E)R'^+(E)G_0^+(0, x'; E), \quad x' < 0, \quad 0 < x < d, \\
 & G^+(x, x'; E) = G_0^+(x, 0; E)T'^+(E)G_0^+(0, x'; E) + \\
 & + G_0^+(x, 0; E)R'^+(E)G_0^+(d, x'; E), \quad 0 < x' < d, \quad x < 0, \\
 & G^+(x, x'; E) = G_0^+(x, x'; E) + \\
 & + G_0^+(x, 0; E)R^+(E)G_0^+(0, x'; E), \quad x' < 0, \quad x < 0, \quad (16)
 \end{aligned}$$

where the transmission and reflection matrices are

$$\begin{aligned}
 T^+(E) &= \frac{T_{><}^{d+}(E)G_0^+(d, 0; E)T_{><}^{0+}(E)}{D^+(E)}, \\
 T'^+(E) &= \frac{T_{><}^{0+}(E)}{D^+(E)}, \\
 R'^+(E) &= T_{<}^{d+}(E)G_0^+(d, 0; E)T'^+(E), \\
 R^+(E) &= T_{<}^{0+}(E) + \\
 &+ \frac{T_{><}^{0+}(E)G_0^+(0, d; E)T_{<}^{d+}(E)G_0^+(d, 0; E)T_{><}^{0+}(E)}{D^+(E)}, \\
 D^+(E) &= 1 - T_{<}^{d+}(E)G_0^+(d, 0; E)T_{>}^{0+}(E)G_0^+(0, d; E).
 \end{aligned} \quad (17)$$

The one-dimensional retarded Green function $G_0^+(x, x'; E)$ corresponding to a free particle moving in a constant potential $V(x) = 0$ or $V(x) = U$ (or Δ) is (see, e.g., [18])

$$\begin{aligned}
 G_0^+(x, x'; E) &= \frac{m}{i\hbar^2 k(E)} \exp[ik(E)|x - x'|], \\
 V(x) = 0, \quad G_0^+(x, x'; E) &= \frac{m}{i\hbar^2 k_{u(\Delta)}(E)} \times \\
 \times \exp[ik_{u(\Delta)}(E)|x - x'|], \quad V(x) = U \text{ (or } \Delta),
 \end{aligned} \quad (18)$$

where the wave numbers are determined by (9). The scattering (at the step located at $x = x_s$) t-matrices are defined by the following perturbation expansion:

$$\begin{aligned}
 T^s(E) &= H_i^s(E) + H_i^s(E)G_0(x_s, x_s; E)H_i^s(E) + \dots = \\
 &= \frac{H_i^s(E)}{1 - G_0(x_s, x_s; E)H_i^s(E)},
 \end{aligned} \quad (19)$$

where $H_i^s(E)$ and the interface Green function $G_0(x_s, x_s; E)$ are defined differently for the reflection and transmission processes [13]: the step-localized effective potential is given by Eq. (15) and the retarded

Green functions at the interface for the considered reflection and transmission processes are, correspondingly,

$$\begin{aligned}
 G_{0>(<)}^+(x_s, x_s; E) &= 1/i\hbar v_{>(<)}^s(E), \\
 G_{0><}^+(x_s, x_s; E) &= 1/i\hbar \sqrt{v_{>}^s(E)v_{<}^s(E)}
 \end{aligned} \quad (20)$$

in accordance with (18).

From (15), (19), and (20), we have $T_{>(<)}^{s+}(E)$ and $T_{><}^{s+}(E)$ t-matrices for the reflection and the transmission, respectively. These matrices are used in (17) ($s \in \{0, d\}$) and correspond to the retarded Green function and the scattering at the interface located at $x = x_s \in \{0, d\}$:

$$\begin{aligned}
 T_{>(<)}^{s+}(E) &= i\hbar v_{>(<)}^s r_{>(<)}^s, \\
 T_{><}^{s+}(E) &= i\hbar \sqrt{v_{>}^s v_{<}^s} t^s,
 \end{aligned} \quad (21)$$

where $r_{>(<)}^s(E)$ and $t^s(E)$ are the standard amplitudes for the reflection to the right (left) of the potential step at $x = x_s$ and the transmission through this step

$$\begin{aligned}
 r_{>}^s(E) &= \frac{k_{>}^s - k_{<}^s}{k_{>}^s + k_{<}^s}, \quad r_{<}^s(E) = \frac{k_{<}^s - k_{>}^s}{k_{>}^s + k_{<}^s}, \\
 t^s(E) &= \frac{2\sqrt{k_{>}^s k_{<}^s}}{k_{>}^s + k_{<}^s}.
 \end{aligned} \quad (22)$$

Here, the argument E is omitted for brevity.

Now, using (9), (16), (17), (18), (21), and (22), we can obtain the Green function $G^+(x, x'; E)$ for the spatial domains considered in (16) (see [17]):

$$\begin{aligned}
 G^+(x, x'; E) &= \frac{m}{i\hbar^2 \sqrt{k k_\Delta}} e^{ik_\Delta(x-d)} t(E) e^{-ikx'}, \\
 x' < 0, \quad x > d, \\
 G^+(x, x'; E) &= \frac{m}{i\hbar^2 \sqrt{k k_\Delta}} e^{-ikx} t(E) e^{ik_\Delta(x'-d)}, \\
 x' > d, \quad x < 0, \\
 G^+(x, x'; E) &= \frac{m}{i\hbar^2 \sqrt{k k_u}} \times \\
 \times \left[e^{ik_u x} t'(E) e^{-ikx'} + e^{-ik_u x} r'(E) e^{-ikx'} \right], \\
 x' < 0, \quad 0 < x < d, \\
 G^+(x, x'; E) &= \frac{m}{i\hbar^2 \sqrt{k k_u}} \times \\
 \times \left[e^{-ikx} t'(E) e^{ik_u x'} + e^{-ikx} r'(E) e^{-ik_u x'} \right], \\
 x < 0, \quad 0 < x' < d,
 \end{aligned}$$

$$G^+(x, x'; E) = \frac{m}{i\hbar^2 k} \left[e^{ik|x-x'|} + r(E)e^{-ik(x+x')} \right],$$

$$x < 0, \quad x' < 0, \quad (23)$$

where the transmission and reflection amplitudes are defined as

$$t(E) = \frac{4\sqrt{k\bar{k}_\Delta k_u} e^{ik_u d}}{d(E)}, \quad t'(E) = \frac{2\sqrt{k\bar{k}_u} (k_\Delta + k_u)}{d(E)},$$

$$r'(E) = \frac{2\sqrt{k\bar{k}_u} (k_u - k_\Delta) e^{2ik_u d}}{d(E)}, \quad (24)$$

$$r(E) = \frac{(k - k_u)(k_\Delta + k_u) - (k + k_u)(k_\Delta - k_u) e^{2ik_u d}}{d(E)},$$

$$d(E) = (k + k_u)(k_\Delta + k_u) - (k - k_u)(k_\Delta - k_u) e^{2ik_u d}.$$

Using the same approach, it is not difficult to obtain the Green function $G^+(x, x'; E)$ for other areas of arguments x and x' .

In accordance with the obtained results for Green's functions, we consider the situation where a particle, given originally by a wave packet localized to the left of the potential area, i.e. at $x' < 0$, moves toward potential (8). We also choose $\Delta \geq 0$, which corresponds to the case where, e.g., the spin-up electrons of the left magnetic layer ($x' < 0$) move through the nonmagnetic spacer to the right magnetic layer ($x > d$) aligned either in parallel ($\Delta = 0$) or antiparallel ($\Delta > 0$) to the left magnetic layer. At the same time, the amplitude U in potential (8) may acquire both positive (barrier) and negative (well) values.

From Eqs. (23), we see that $G^+(x, x'; E) = G^+(x', x; E)$, and, therefore, the advanced Green function $G^-(x, x'; E) = [G^+(x', x; E)]^* = [G^+(x, x'; E)]^*$ (see, e.g., [18]). Thus, the transmission amplitude (12) is determined by the imaginary part of the Green function and can be written as

$$K(x, x'; t) = -\theta(t) \frac{1}{\pi} \int_{-\infty}^{\infty} dE e^{-\frac{i}{\hbar} Et} \text{Im} G^+(x, x'; E). \quad (25)$$

Formulas (23)–(25) present the exact solution for the particle propagator in the presence of potential (8). It should be kept in mind that the wave numbers (9) and, therefore, the quantities $t(E)$, $t'(E)$, $r'(E)$, and $r(E)$ in (24) are different in the $\int_{-\infty}^0 dE$ and $\int_0^{\infty} dE$ energy integration areas: in the former case, $k(E)$ and $k_\Delta(E)$ ($\Delta \geq 0$) should be replaced with $i\bar{k}(E)$ and $i\bar{k}_\Delta(E)$, where $\bar{k}(E) = \sqrt{-2mE/\hbar^2}$ ($E < 0$) and $\bar{k}_\Delta(E) = \sqrt{2m(\Delta - E)/\hbar^2}$. At the same

time, for energies $E < 0$, the wave number $k_u = i\bar{k}_u$, $\bar{k}_u = \sqrt{2m(U - E)/\hbar^2}$, for $U > 0$ (barrier), but it is real for $U < 0$, i.e. $k_u = \sqrt{2m(E + |U|)/\hbar^2}$, if $E > -|U|$ and $k_u = i\bar{k}_u$, $\bar{k}_u = \sqrt{-2m(E + |U|)/\hbar^2}$ if $E < -|U|$. It follows that the “free” Green function $G_0^+(x, x'; E) = \frac{m}{i\hbar^2 k} e^{ik|x-x'|}$ is real in the energy interval $(-\infty \div 0)$ and, therefore, does not contribute in this interval to the corresponding “free” propagator $K_0(x, x'; t)$ defined by (25). It is also remarkable that, for energies $E < 0$, the imaginary parts of the Green functions vanish in all spatial regions, as is seen from definitions (23) and (24) (e.g., $\text{Im} t(E) = 0$ and $\text{Im} r(E) = 0$ for $E < 0$). Therefore, the energy interval $(-\infty \div 0)$ does not contribute to the propagation of the particles through the potential well/barrier region. Thus, we have, for $t > 0$,

$$K(x, x'; t) = \frac{1}{\pi\hbar} \int_0^{\infty} dE e^{-\frac{i}{\hbar} Et} \times$$

$$\times \text{Re} \left[\frac{t(E) e^{ik_\Delta(E)(x-d)} e^{-ik(E)x'}}{\sqrt{v_\Delta(E)}} \right], \quad x' < 0, \quad x > d,$$

$$K(x, x'; t) = \frac{1}{\pi\hbar} \int_0^{\infty} dE e^{-\frac{i}{\hbar} Et} \times$$

$$\times \text{Re} \left\{ \frac{e^{-ik(E)x'} [t'(E) e^{ik_u(E)x} + r'(E) e^{-ik_u(E)x}]}{\sqrt{v_u(E)}} \right\}, \quad (26)$$

$$x' < 0, \quad 0 < x < d,$$

$$K(x, x'; t) = \frac{1}{\pi\hbar} \int_0^{\infty} dE e^{-\frac{i}{\hbar} Et} \frac{\text{Re}[e^{ik(E)|x-x'|} +$$

$$+ r(E) e^{-ik(E)(x+x')}]}, \quad x' < 0, \quad x < 0,$$

where the velocities $v(E)$, $v_u(E)$, and $v_\Delta(E)$ are defined by (9) with the multiplier \hbar/m .

It is easy to verify that the integration of the first term in the last line of (26) over E results in the known formula for the space-time propagator of a freely moving particle

$$K_0(x, x'; t) = \left(\frac{m}{2\pi i\hbar t} \right)^{1/2} \times$$

$$\times \exp \left[\frac{im(x - x')^2}{2\hbar t} \right], \quad x < 0, \quad x' < 0. \quad (27)$$

The obtained results (26) for the particle propagator completely resolve (by means of Eq. (3)) the time-dependent Schrödinger equation for a particle

moving under the influence of the rectangular potential (8). The form of this solution (integrals of elementary functions) is convenient for a numerical visualization. The further application of these results to the calculation of the TOA and dwell time, as well as of the probability density of finding a particle in different spatial areas as a function of the time with account for the forward- and backward-moving components of the wave function and their interference, can be found in our earlier papers [13–15, 17].

3. Application to the Density Matrix

The equilibrium non-normalized density operator (propagator in the temperature domain) $\rho(\beta) = \exp(-\beta H)$ can likewise be expressed in terms of the resolvent operator $(E - H)^{-1}$ (see (10)) as

$$\rho(\beta) = \exp(-\beta H) = \frac{i}{2\pi} \int_{-\infty}^{\infty} dE e^{-\beta E} \times \left(\frac{1}{E - H + i\varepsilon} - \frac{1}{E - H - i\varepsilon} \right). \quad (28)$$

Particularly, in the coordinate representation, the density matrix takes the form (see (4))

$$\rho(x, x'; \beta) = \int_{-\infty}^{\infty} e^{-\beta E} A(x, x'; E) dE, \quad (29)$$

where $A(x, x'; E)$ is given by (13). Thus, the density matrix $\rho(x, x'; \beta)$ follows from propagator (12) by the substitution $t \rightarrow -i\hbar\beta$ ($\beta = 1/k_B T$). From properties (13), we see that the density matrix (29) is self-adjoint. The density operator (28) satisfies the Bloch equation (5).

Thus, passing to the imaginary “time” ($t \rightarrow -i\hbar\beta$), we obtain the exact density matrix $\rho(x, x'; \beta)$ in the various considered (relative to potential (8) area) spatial regions, i.e.,

$$\rho(x, x'; \beta) = K(x, x'; -i\hbar\beta), \quad (30)$$

where $K(x, x'; t = -i\hbar\beta)$ is given by (26). In particular, formula (27) yields the known result for the “free” density matrix

$$\begin{aligned} \rho_0(x, x'; \beta) &= K_0(x, x'; -i\hbar\beta) = \\ &= \left(\frac{m}{2\pi\hbar^2\beta} \right)^{1/2} \exp \left[-\frac{m(x - x')^2}{2\hbar^2\beta} \right]. \end{aligned} \quad (31)$$

Using the same approach, it is not difficult to obtain the propagator $\rho(x, x'; \beta)$ for other (than in (26)) areas of the arguments x and x' . Again, it is worth to note that the negative-energy half-line ($-\infty \div 0$) corresponding to the evanescent states does not contribute to propagator (29). The diagonal element $K(x, x; \beta)$ ($x = x'$ can be put only in the last line of (26)) defines the density of particles per unit length at the point $x < 0$ to the left of potential (8). The nondiagonal elements $K(x, x'; \beta)$ of (26) are related to the quantum mechanical interference effects. Particularly, they are responsible for the particle tunneling through the barrier and also can be attributed to the phase correlation of the states $|x\rangle$ and $|x'\rangle$.

Equations (26) and (30) provide the exact solution for the particle density matrix in the presence of the rectangular potential (8) in terms of integrals of elementary functions. It is convenient (e.g., for a numerical visualization of the obtained results) to pass to dimensionless variables. As seen from (8), (9), and (26), there are the natural spatial scale d and the energy scale $E_d = \hbar^2/2md^2$ (the energy uncertainty due to the particle localization within a potential range of width d). Then the density matrix (30) in the different spatial regions can be presented in the dimensionless variables as

$$\begin{aligned} \rho(\tilde{x}, \tilde{x}'; \tilde{\beta}) &= \frac{1}{2\pi d} \int_0^{\infty} \frac{d\tilde{E} e^{-\tilde{\beta}\tilde{E}}}{\tilde{E}^{1/4}} \times \\ &\times \operatorname{Re} \left[\frac{\tilde{t}(\tilde{E}) e^{i\sqrt{\tilde{E}-\tilde{\Delta}}(\tilde{x}-1)} e^{-i\sqrt{\tilde{E}}\tilde{x}'}}{(\tilde{E}-\tilde{\Delta})^{1/4}} \right], \quad \tilde{x}' < 0, \tilde{x} > 1, \\ \rho(\tilde{x}, \tilde{x}'; \tilde{\beta}) &= \frac{1}{2\pi d} \int_0^{\infty} \frac{d\tilde{E} e^{-\tilde{\beta}\tilde{E}}}{\tilde{E}^{1/4}} \times \\ &\times \operatorname{Re} \left\{ \frac{[\tilde{t}'(\tilde{E}) e^{i\sqrt{\tilde{E}-\tilde{U}}\tilde{x}} + \tilde{r}'(\tilde{E}) e^{-i\sqrt{\tilde{E}-\tilde{U}}\tilde{x}}] e^{-i\sqrt{\tilde{E}}\tilde{x}'}}{(\tilde{E}-\tilde{U})^{1/4}} \right\}, \\ &\tilde{x}' < 0, 0 < \tilde{x} < 1, \\ \rho(\tilde{x}, \tilde{x}'; \tilde{\beta}) &= \frac{1}{2\sqrt{\pi\tilde{\beta}d}} \exp[-(\tilde{x} - \tilde{x}')^2/4\tilde{\beta}] + \\ &+ \frac{1}{2\pi d} \int_0^{\infty} \frac{d\tilde{E} e^{-\tilde{\beta}\tilde{E}}}{\sqrt{\tilde{E}}} \operatorname{Re}[\tilde{r}(\tilde{E}) e^{i\sqrt{\tilde{E}}(\tilde{x}+\tilde{x}')}], \\ &\tilde{x}' < 0, \tilde{x} < 0, \end{aligned} \quad (32)$$

where

$$\begin{aligned}
 \tilde{t}(\tilde{E}) &= \frac{4\tilde{E}^{1/4}(\tilde{E} - \tilde{\Delta})^{1/4}\sqrt{\tilde{E} - \tilde{U}}e^{i\sqrt{\tilde{E} - \tilde{U}}}}{\tilde{d}(\tilde{E})}, \\
 \tilde{t}'(\tilde{E}) &= \frac{2\tilde{E}^{1/4}(\tilde{E} - \tilde{U})^{1/4}(\sqrt{\tilde{E} - \tilde{\Delta}} + \sqrt{\tilde{E} - \tilde{U}})}{\tilde{d}(\tilde{E})}, \\
 \tilde{r}'(\tilde{E}) &= \frac{2\tilde{E}^{1/4}(\tilde{E} - \tilde{U})^{1/4}(\sqrt{\tilde{E} - \tilde{U}} - \sqrt{\tilde{E} - \tilde{\Delta}})e^{2i\sqrt{\tilde{E} - \tilde{U}}}}{\tilde{d}(\tilde{E})}, \\
 \tilde{r}(\tilde{E}) &= \{(\sqrt{\tilde{E} - \tilde{U}} - \sqrt{\tilde{E} - \tilde{\Delta}})(\sqrt{\tilde{E} - \tilde{\Delta}} + \sqrt{\tilde{E} - \tilde{U}} - \\
 &\quad - (\sqrt{\tilde{E} + \sqrt{\tilde{E} - \tilde{U}}})(\sqrt{\tilde{E} - \tilde{\Delta}} - \sqrt{\tilde{E} - \tilde{U}}) \times \\
 &\quad \times e^{2i\sqrt{\tilde{E} - \tilde{U}}}\}/\tilde{d}(\tilde{E}), \\
 \tilde{d}(\tilde{E}) &= (\sqrt{\tilde{E} + \sqrt{\tilde{E} - \tilde{U}}})(\sqrt{\tilde{E} - \tilde{\Delta}} + \sqrt{\tilde{E} - \tilde{U}}) - \\
 &\quad - (\sqrt{\tilde{E} - \sqrt{\tilde{E} - \tilde{U}}})(\sqrt{\tilde{E} - \tilde{\Delta}} - \sqrt{\tilde{E} - \tilde{U}})e^{2i\sqrt{\tilde{E} - \tilde{U}}}, \tag{33}
 \end{aligned}$$

and $\tilde{E} = E/E_d$, $\tilde{U} = U/E_d$, $\tilde{\Delta} = \Delta/E_d$, $\tilde{\beta} = E_d/k_B T = \tilde{T}/T$, $\tilde{T} = E_d/k_B$, $\tilde{x} = x/d$, $\tilde{x}' = x'/d$.

We will visualize the results given by Eqs. (32) and (33) for several specific values of the relevant parameters. For an electron and the potential width $d = 10^{-7}$ cm (1 nm), the characteristic energy $E_d \sim 3 \times 10^{-2}$ eV and the characteristic temperature $\tilde{T} = E_d/k_B \sim 3 \times 10^2$ K.

We will perform the numerical modeling of the density matrix (32) with the symmetric rectangular potential (8) for $\Delta = 0$ (in this case, the transition and reflection amplitudes (33) are simplified essentially). To secure a rapid convergence of the integrals in (32), we consider low enough temperatures, i.e., put $\tilde{\beta} = 10$ ($k_B T \ll E_d$). Figure 1 shows the diagonal element of the density matrix $\rho(\tilde{x}, \tilde{x}; \tilde{\beta})$ (the last line in (32)) at $\tilde{x} = -2$, i.e., the probability density to find a particle at this spatial point to the left of the barrier as a function of the potential well modulus $|\tilde{U}|$ ($\tilde{U} = 0 \div -300$). We see that, in this case, the density matrix $\rho(\tilde{x}, \tilde{x}; \tilde{\beta})$ exhibits a series of maxima and minima. This can be explained by the formation of resonance levels above the well, if the condition $\tilde{E} + |\tilde{U}| = \pi^2 n^2$ (n is integer, $n = 1, 2, \dots$) holds. With such a condition, we have the reflection

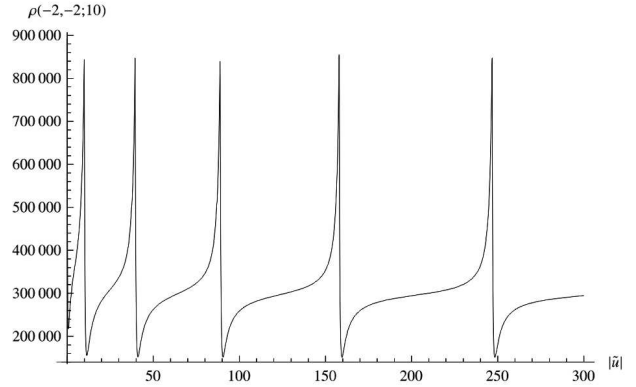


Fig. 1. Diagonal element $\rho(-2, -2; 10)$ as a function of the potential well depth $|\tilde{U}|$

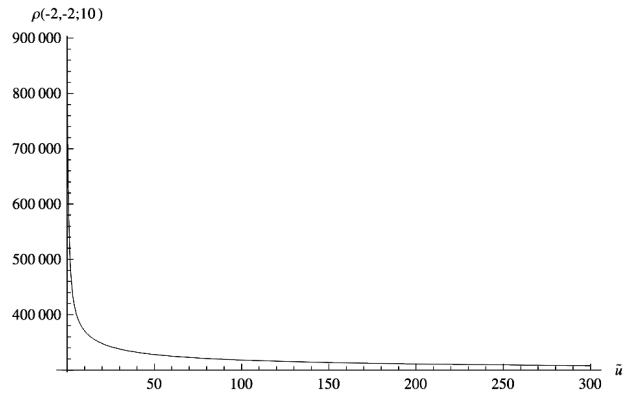


Fig. 2. The same (as in Fig. 1) diagonal element of the density matrix as a function of the potential barrier height \tilde{U}

amplitude $\tilde{r}(\tilde{E}) = 0$ and the transmission amplitude $\tilde{t}(\tilde{E}) = \pm 1$. As the main contribution to the integral over \tilde{E} at low temperatures ($\tilde{\beta} = 10$) comes from the small (close to zero) energies, the positions of jumps in Fig. 1 approximately follow the relation $|\tilde{U}| = \pi^2 n^2$ ($n = 1, 2, \dots$).

The same diagonal element $\rho(-2, -2; 10)$ as a function of the height of the potential barrier $\tilde{U} = 0 \div 300$ behaves quite different from the case of the potential well and is shown in Fig. 2. One can see that the particle probability density at the given point to the left of the barrier $\tilde{x} = -2$ exhibits, at first, a step fall with the potential barrier growth, and then it changes slowly with \tilde{U} .

We will evaluate the nondiagonal elements of the density matrix $\rho(\tilde{x}, \tilde{x}'; \tilde{\beta})$ for points on different sides of the well/barrier (the first line in (32)) as a function

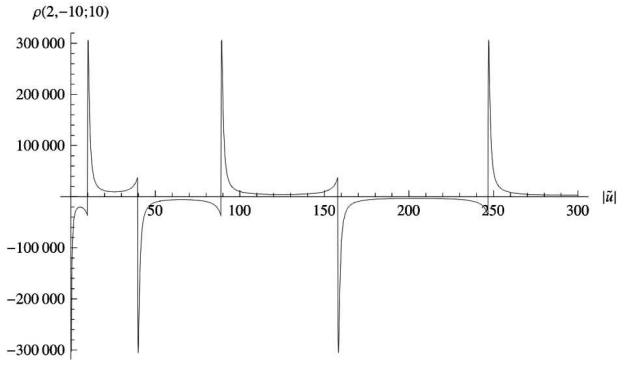


Fig. 3. Nondiagonal element of the density matrix $\rho(2, -10; 10)$ as a function of the potential well depth $|\tilde{U}|$

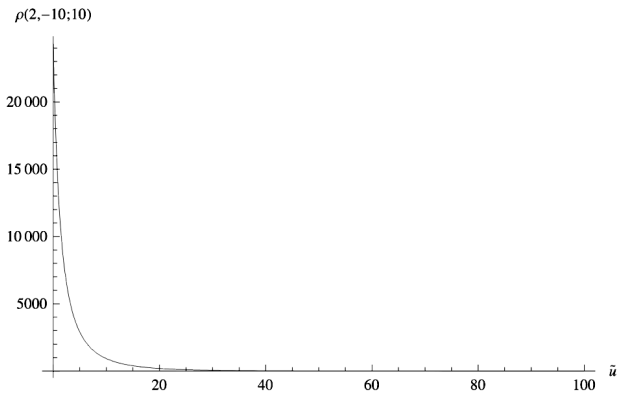


Fig. 4. Dependence of $\rho(2, -10; 10)$ on the potential barrier height \tilde{U}

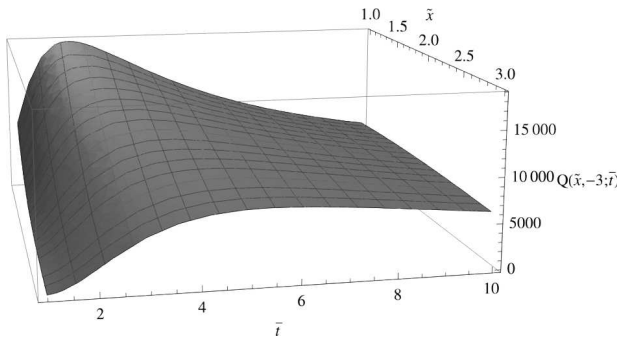


Fig. 5. Three-dimensional profile of the particle density $Q(\tilde{x}, -3; \tilde{t})$ to the right of the symmetric barrier

of the potential parameter \tilde{U} . Thus, we put $\tilde{x}' = -10$ (before the potential), $\tilde{x} = 2$ (beyond the potential) and $\tilde{\beta} = 10$ (as for Figs. (8) and (9)). Figure 3 exhibits the peaks of the density matrix in the case of the potential well with $\tilde{U} = 0 \div -300$ at the reso-

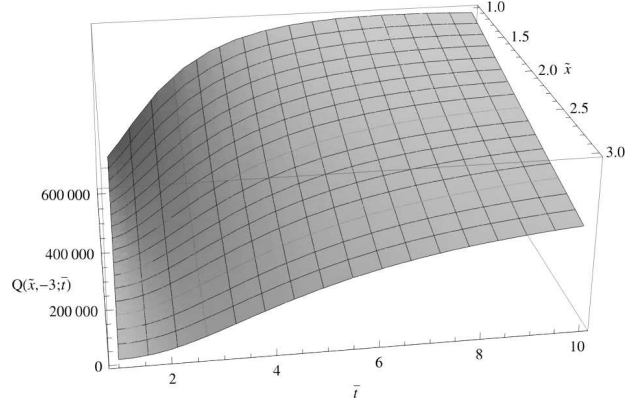


Fig. 6. Space-time density profile $Q(\tilde{x}, -3; \tilde{t})$ for the "free" diffusion of particles

nance values of $|\tilde{U}|$, which correspond to the minima in Fig. 1.

We see that, in this case ($\tilde{U} < 0$), the nondiagonal elements of the density matrix can acquire both positive and negative values. Note that, at $\tilde{U} = 0$, the density matrix reduces to the free density matrix (31) and, therefore, is positive (the seemingly negative value of the density matrix close to $\tilde{U} = 0$ in Fig. 3 is due to a small resolution on the $|\tilde{U}|$ -axis; the calculation on the smaller scale near the point $\tilde{U} = 0$ shows that, at $\tilde{U} = 0$, the density matrix is positive). Thus, Fig. 3 demonstrates the jumps of the quantum coherence between the particle states before ($x' < 0$) and beyond ($x > 0$) the potential well at the resonance particle transmission through the potential well. At the values of $|\tilde{U}|$ that do not satisfy the resonance condition, this quantum coherence is small.

The nondiagonal matrix element $\rho(2, -10; 10)$ as a function of the potential barrier height ($\tilde{U} = 0 \div 100$) is shown in Fig. 4. We see that the quantum coherence between the states on the different sides of the barrier goes quickly enough to zero, as the barrier height increases.

4. Diffusion-Like Equation

As was mentioned in Introduction, the time-dependent Schrödinger equation (1) becomes equivalent to the parabolic diffusion-like equation (6), if one makes the substitutions $t \rightarrow -it$ and $\hbar \rightarrow 2mD$, where D is a (diffusion) constant. From Eqs. (26), we can immediately obtain a solution to the diffusion equation (6) under the initial condition $Q(x; 0) = \delta(x - x')$. In the

dimensionless variables, this solution (a propagator) is given by Eqs. (32) and (33) with the substitutions

$$\begin{aligned} \rho(\tilde{x}, \tilde{x}'; \tilde{\beta}) &\rightarrow Q(\tilde{x}, \tilde{x}'; \tilde{t}), \quad \tilde{\beta} \rightarrow \tilde{t}, \quad \tilde{E} \rightarrow \bar{E}, \\ \tilde{U} &\rightarrow \bar{U}, \quad \tilde{\Delta} \rightarrow \bar{\Delta}, \quad \tilde{t} = t/t_D, \quad \bar{E} = E/E_D, \\ \bar{U} &= U/E_D, \quad \bar{\Delta} = \Delta/E_D, \\ t_D &= d^2/D, \quad E_D = 2mD^2/d^2, \end{aligned} \quad (34)$$

where t_D and E_D are obtained from t_d and E_d of the previous section by the substitution $\hbar \rightarrow 2mD$. As follows from definition (34), the introduced characteristic time t_D can be interpreted as the time needed for a particle to diffuse over the distance d (width of potential (8)) with the diffusion coefficient D . The characteristic energy $E_D = 2mD^2/d^2 = 2md^2/t_D^2 = 4\frac{mv_D^2}{2}$ is proportional to the kinetic energy of a particle moving with the average velocity $v_D = d/t_D$. Therefore, as in the previous section, we can numerically model the solution $Q(\tilde{x}, \tilde{x}'; \tilde{t})$ defined by Eqs. (32) and (33) (with substitutions (34)) at the different spatial points $\tilde{x} = x/d$ and $\tilde{x}' = x'/d$.

Note that, at $\bar{V}(x) > 0$, the solution to the diffusion equation (6) is positive, $Q(\tilde{x}, \tilde{x}'; \tilde{t}) \geq 0$ (see [8]) and can be viewed as the density of particles at the point \tilde{x} at the time moment \tilde{t} , when the “diffusion with holes” starts at the point \tilde{x}' . The latter term was introduced by Kac because, at the points, where potential (8) $\bar{V}(x) \neq 0$ ($\bar{V}(x) > 0$), the particle can disappear.

As an example, we have numerically modeled the density of particles $Q(\tilde{x}, \tilde{x}'; \tilde{t})$ to the right of the symmetric barrier ($\Delta = 0$) with $\bar{U} = 10$ at different \tilde{x} , when the diffusion starts to the left of the barrier at $\tilde{x}' < 0$. The chosen scaled time $\tilde{t} = 1 \div 10$ is sufficient to reach the spatial domain $\tilde{x} = 1 \div 3$ starting at $\tilde{x}' = -3$. The calculated three-dimensional profile of $Q(\tilde{x}, \tilde{x}'; \tilde{t})$ is presented in Fig. 5 for the same (as earlier) width of the potential barrier $d = 10^{-7}$ cm.

One can see the nonmonotonic behavior of the density profile with time \tilde{t} for every fixed \tilde{x} , which is especially pronounced near the right barrier boundary (near $\tilde{x} = 1$). This behavior caused by the negative sources absorbing the particles (see Eq. (6)) and distributed according to function (8) with $U > 0$, $\Delta = 0$, is quite different from the familiar “free” diffusion in the absence of the potential ($U = 0$, $\Delta = 0$),

which is shown in Fig. 6 for the same parameters as in Fig. 5.

5. Summary

We have obtained the exact propagator $\langle x | \exp(-\alpha H) | x' \rangle$ (H is the Hamiltonian for a particle moving in the presence of an asymmetric rectangular potential) resolving the parabolic-type partial differential equation. Having obtained the space-time propagator for the one-dimensional time-dependent Schrödinger equation ($\alpha = it/\hbar$) with a rectangular well/barrier potential, we succeeded, at the same time, in finding a propagator for the Bloch equation ($\alpha = \beta$, $\beta = 1/k_B t$) for the particle density matrix and for the diffusion-like equation ($\alpha = t$) by passing from the real to the imaginary time ($t \rightarrow -i\hbar\beta$ and $t \rightarrow -it$, correspondingly). As an alternative to the conventional path integral approach to calculating the propagators, we use the multiple-scattering theory for the calculation of the energy-dependent Green function (a resolvent operator in (10)). The suggested approach is based on the possibility of introducing the effective potentials (see (14) and (15)), which are responsible for the reflection from and the transmission through the potential jumps making up the rectangular potential (8). It provides more of a non-classical picture of particle scattering at the considered potential as opposed to the conventional wave point of view.

The solution for the time-dependent Schrödinger equation describes the reflection from and the transmission through an asymmetric rectangular potential as a function of the time and thus allows the consideration of the non-classical counterintuitive effects of the particle reflection from a potential well and the transmission through a potential barrier in a real situation where a particle is moving toward potential (8) and then experiencing a scattering at the potential. These results are also relevant to the fundamental issues of measuring the time in quantum mechanics such as the time-of-arrival (TOA), dwell time, and tunneling time.

The obtained density matrix $\rho(x, x'; \beta)$ for a particle in a heat bath and under the influence of potential (8) gives the probability density (diagonal matrix element) to find a particle at some spatial point and the quantum correlation (coherence) of different spatial

states $|x\rangle$ and $|x'\rangle$ provided by the nondiagonal matrix elements. The results for the density matrix are numerically visualized, which is enabled by the fact that they are expressed in terms of integrals of elementary functions.

The results of the solution of the diffusion-like equation, which can be interpreted (in the case of a potential barrier, $U > 0$) as the diffusion with negative sources distributed according to potential (8), also have been numerically evaluated. The corresponding figures demonstrate the difference between this “diffusion with holes” and the “free” diffusion in the absence of potential (8).

It is also worth mentioning that all obtained results are also relevant to the properties of electrons in nanostructures important for spintronics devices, because potential (8) can be used for modeling the potential profiles in such materials.

1. A.D. Baute, I.L. Egusquiza, and J.G. Muga, *J. Phys. A: Math. Theor.* **34**, 42892001 (2001).
2. A.D. Baute, I.L. Egusquiza, and J.G. Muga, *Int. J. Theor. Physics, Group Theory, and Nonlinear Optics* **8**, 1 (2002); (e-print arXiv: quant-ph/0007079).
3. *Time in Quantum Mechanics, vol. 1 (Lecture Notes in Physics, vol. 734)*, edited by J.G. Muga, R. Sala Mayato, and I.L. Egusquiza (Springer, Berlin, 2008).
4. *Time in Quantum Mechanics, vol. 2 (Lecture Notes in Physics, vol. 789)*, edited by J.G. Muga, A. Ruschhaupt, and A. del Campo (Springer, Berlin, 2009).
5. M.N. Baibich, J.M. Broto, A. Fert, F. Nguyen Van Dau, F. Petroff, P. Etienne, G. Creuzet, A. Friederich, and J. Chazelas, *Phys. Rev. Lett.* **61**, 2472 (1988).
6. R. Julliere, *Phys. Lett. A* **54**, 225 (1975); P. LeClair, J.S. Moodera, and R. Meservay, *J. Appl. Phys.* **76**, 6546 (1994).
7. R.P. Feynman and A.R. Hibbs, *Quantum Mechanics and Path Integrals* (McGraw-Hill, New York, 1965).
8. M. Kac, *Probability and Related Topics in Physical Sciences, Lectures in Applied Mathematics, vol. 1* (Interscience, London, New York, 1958).
9. A.O. Barut and I.H. Duru, *Phys. Rev. A* **38**, 5906 (1988).
10. L.S. Schulman, *Phys. Rev. Lett.*, **49**, 599 (1982).
11. T.O. de Carvalho, *Phys. Rev. A* **47**, 2562 (1993).
12. J.M. Yearsley, *J. Phys. A: Math. Theor.* **41**, 285301 (2008).
13. V.F. Los and A.V. Los, *J. Phys. A: Math. Theor.* **43**, 055304 (2010).
14. V.F. Los and A.V. Los, *J. Phys. A: Math. Theor.* **44**, 215301 (2011).
15. V.F. Los and M.V. Los, *J. Phys. A: Math. Theor.* **45**, 095302 (2012).
16. J.G. Muga and C.R. Leavens, *Phys. Rep.* **338**, (2000).

17. V.F. Los and M.V. Los, *Theor. Math. Phys.* **177**, 1704 (2013).

18. E.N. Economou, *Green's Functions in Quantum Physics* (Springer, Berlin, 1979).

Received 10.06.15

В.Ф. Лось, М.В. Лось

ТОЧНЕ РІШЕННЯ ЗАЛЕЖНОГО ВІД ЧАСУ РІВНЯННЯ ШРЕДІНГЕРА З ПРЯМОКУТНИМ ПОТЕНЦІАЛОМ ДЛЯ ДІЙСНОГО І УЯВНОГО ЧАСУ

Резюме

Використовуючи теорію багатократного розсіяння, отримано пропагатор для одновимірною, залежного від часу рівняння Шредінгера з асиметричним прямокутним потенціалом. Це дозволило розглядати процеси відбивання і проходження, як розсіяння частинки на стрибках потенціалу (на відміну від звичайної хвильової картини), та враховувати неklasичний і парадоксальний внесок обернено рухомих компонент хвильового пакета, що асоціюється із частинкою. Отриманий пропагатор дає повне рішення відповідного залежного від часу рівняння Шредінгера (тобто визначає хвильову функцію $\psi(x, t)$) та дозволяє розгляд квантово-механічних ефектів відбивання частинки від потенціальної ями (або сходинки) та її проходження через потенціальний бар'єр як функцію часу. Ці результати стосуються таких фундаментальних проблем, як вимір часу у квантовій механіці (час тунелювання, час прибуття, час перебування). Для уявного часу, що представляє обернену температуру ($t \rightarrow -i\hbar/k_B T$), отриманий пропагатор є еквівалентним до матриці густини для частинки, яка знаходиться у термостаті і під впливом прямокутного потенціалу. Ця матриця густини надає інформацію про густину частинок у різних просторових областях (відносно розташування потенціалу) і про квантову когерентність різних просторових станів частинки. Якщо перейти до уявного часу, як $t \rightarrow -it$, то матричний елемент обчисленого пропагатора у просторовому базисі дає рішення рівняння дифузійного типу з прямокутним потенціалом. Отримані точні результати представлені у вигляді інтегралів від елементарних функцій, і таким чином дозволяють чисельно візуалізувати густину ймовірності $|\psi(x, t)|^2$, матрицю густини та рішення рівняння дифузійного типу. Отримані результати можуть також бути корисними для спінтроники, оскільки асиметричний (залежний від спіну) прямокутний потенціал моделює потенціальний профіль шаруватих магнітних наноструктур.

В.Ф. Лось, Н.В. Лось

ТОЧНОЕ РЕШЕНИЕ ВРЕМЕННОГО УРАВНЕНИЯ ШРЕДИНГЕРА С ПРЯМОУГОЛЬНЫМ ПОТЕНЦИАЛОМ ДЛЯ ДЕЙСТВИТЕЛЬНОГО И МНИМОГО ВРЕМЕНИ

Резюме

Используя теорию многократного рассеяния, получен пропагатор для одномерного временного уравнения Шредингера с асимметричным прямоугольным потенциалом. Это

позволило рассматривать процессы отражения и прохождения как рассеяние частицы на скачках потенциала (в отличие от обычной волновой картины) и учитывать неклассический парадоксальный вклад движущихся в обратном направлении компонент волнового пакета, который ассоциируется с частицей. Полученный пропагатор дает полное решение соответствующего временного уравнения Шредингера (т.е. определяет волновую функцию $\psi(x, t)$) и позволяет рассматривать квантово-механические эффекты отражения частицы от потенциальной ямы (или ступеньки), а также ее прохождение через потенциальный барьер как функцию времени. Эти результаты касаются таких фундаментальных проблем, как измерение времени в квантовой механике (время туннелирования, время прибытия, время пребывания). Для мнимого времени, которое представляет обратную температуру ($t \rightarrow -i\hbar/k_B T$), полученный пропагатор эквивалентен матрице плотности для частицы, находящейся в термостате и под влиянием прямоугольного потенциала. Эта матрица плотности дает информацию о плотности частиц в разных пространственных областях (относительно положения потенциала) и о квантовой когерентности разных пространственных состояний частиц. Если перейти к мнимому времени $t \rightarrow -it$, то матричный элемент полученного пропагатора в пространственном базисе дает решение уравнения диффузионного типа с прямоугольным потенциалом. Полученные точные результаты представлены в виде интегралов от элементарных функций и таким образом позволяют численно визуализировать плотность вероятности $|\psi(x, t)|^2$, матрицу плотности и решение уравнения диффузионного типа. Полученные результаты могут также быть полезными для спинтроники, поскольку асимметричный (зависящий от спина) прямоугольный потенциал моделирует потенциальный профиль слоистых магнитных наноструктур.

дующейся в термостате и под влиянием прямоугольного потенциала. Эта матрица плотности дает информацию о плотности частиц в разных пространственных областях (относительно положения потенциала) и о квантовой когерентности разных пространственных состояний частиц. Если перейти к мнимому времени $t \rightarrow -it$, то матричный элемент полученного пропагатора в пространственном базисе дает решение уравнения диффузионного типа с прямоугольным потенциалом. Полученные точные результаты представлены в виде интегралов от элементарных функций и таким образом позволяют численно визуализировать плотность вероятности $|\psi(x, t)|^2$, матрицу плотности и решение уравнения диффузионного типа. Полученные результаты могут также быть полезными для спинтроники, поскольку асимметричный (зависящий от спина) прямоугольный потенциал моделирует потенциальный профиль слоистых магнитных наноструктур.